43rd AIAA/ASME/SAE/ASEE Joint Propulsion Conference & Exhibit
8 - 11 July 2007, Cincinnati, OH

AIAA 2007-5026

Evaluation of Oblique and Traverse Fuel Injection in a Supersonic Combustor

A. Abdelhafez* **and A. K. Gupta†**
Department of Mechanical Engineering, University of Maryland
College Park, MD 20742

R. Balar‡ **and K. H. Yu§**
Department of Aerospace Engineering, University of Maryland
College Park, MD 20742

The oblique and traverse configurations of injecting gaseous fuel in a low-aspect-ratio supersonic combustor are characterized and compared numerically using a validated code. Non-reacting conditions are considered, where fuel is simulated by helium. The combustor, which has a rectangular cross-section of constant span, is attached to a Mach 2 nozzle and expands along the top and bottom walls. A choked wall port is used for both injection configurations. Different sets of operating conditions have been simulated. It was found that injecting fuel obliquely results in higher efficiency as well as effectiveness. Unlike the traverse configuration, oblique injection makes use of the beneficial interaction of the injection-induced shock waves with the air/fuel shear layer. This interaction was proven in previous research to be effective for mixing enhancement in supersonic flows. However, in contrast with the results of previous research, normal or oblique injection at large angles (30° or 60°) is not necessary for the achievement of sufficient mixing in supersonic flows. Substantial mixing improvement was found at angles as small as 5°. Fuel injection at such small angles improves the fuel-air mixing while minimizing the injection-induced pressure losses, which leads to increased thrust. Our results on mixing under non-reacting conditions provide good preliminary insights on a more favorable fuel injection configuration that provides better mixing with lower losses and higher thrust.

I. Introduction

ALTHOUGH scramjet-engine-powered vehicles are the future of high-speed flight, mixing and ignition in such engines still need extensive investigation, in order to achieve full understanding of the complicated flow dynamics and chemistry involved. Efficient mixing, ignition, and combustion are necessary for the successful operation of any air-breathing system.[1] The efficiency and effectiveness of an injection system are defined by the degree of fuel/air mixing and the system capability of minimizing injection-induced thrust losses, respectively.[2] In many instances, the equivalence ratio of operation has to be fuel-rich to ensure that a flame is present to provide positive thrust. Therefore, any progress made on improving the engine efficiency must be closely followed towards achieving efficient mixing between fuel and air. Scramjet flows have residence times of of the order of a millisecond. Within that short residence time, the mixing, ignition delay, and combustion time scales should be accounted for. Figure 1 shows how challenging it is to achieve this. Plotted are the temporal variations of temperature for different H_2/air equivalence ratios inside a perfectly-stirred reactor. Fuel-rich conditions are considered, as is the case for actual scramjet engines. Perfect mixing is assumed, i.e., hydrogen mixes instantaneously and homogeneously over the entire reactor after injection. An inlet air temperature of 1000 K is chosen as a common representative of the conditions after the inlet and isolator sections of a hypersonic vehicle. Constant combustor pressure is assumed throughout at 1 atm. It can be seen from Figure 1 that the ignition delay increases from 0.25 to 1.00 ms with increasing equivalence ratio, whereas combustion has an almost fixed time scale of about 0.2 ms. The average value of ignition delay agrees well with the findings of previous research.[3,4] If the assumption of a perfectly-stirred reactor is relieved, the mixing time scale and mixture non-homogeneity will have to be accounted for. This imposes more challenges, if a target residence time of about 1 ms is sought. Failure to meet such strict demands reflects on the combustor length, which, in turn, affects the vehicle weight, available payload, developed thrust, and specific impulse.

Previous research has shown that flame holding in reacting supersonic flows is achieved by creating a recirculation zone, where fuel and air are partially mixed at low velocities.[5] In case of traverse (normal) fuel injection from a

* Graduate Student, Student Member AIAA
† Professor, Fellow AIAA, email: akgupta@eng.umd.edu
‡ Graduate Research Assistant, Student Member AIAA
§ Associate Professor, Associate Fellow AIAA

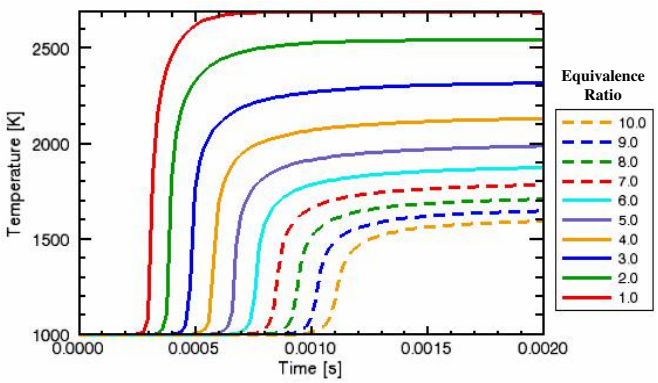

Figure 1. Temporal temperature variation of a perfectly-stirred constant-pressure closed H_2/air reactor. Initial air temperature = 1000 K, reactor pressure = 1 atm.

wall orifice, a bow shock is formed as a result of the direct interaction of fuel jet and supersonic crossflow of air, see Figure 2. Consequently, the upstream wall boundary layer separates, providing a region where the boundary layer and fuel jet mix subsonically upstream of the jet exit. This region was reported to be important in the traverse-injection flowfield because of its flame-holding capability under reacting conditions. Several studies have been conducted on this region.[6,7] Autoignition was observed at the jet upstream recirculation region and behind the bow shock. However, this injection configuration does not provide the sought full penetration of fuel into the supersonic crossflow of air. Furthermore, it has significant stagnation pressure losses due to the strong three-dimensional bow shock[8] formed by the traverse jet penetration. On the other hand, it is possible to increase the injection system effectiveness, i.e., reduce the injection-induced total pressure losses, by using angled (oblique) injection. A weaker bow shock results; see Figure 2. In this configuration, the fuel jet axial momentum can also contribute to the net engine thrust.

In an experimental investigation[9], a supersonic hydrogen flame, with coaxial injection, was stabilized successfully along the axis of a Mach 2.5 wind tunnel. Stabilization was achieved by using small-angled wedges mounted on the tunnel sidewalls to generate weak oblique shock waves that interact with the flame. It was found that these shock waves enhance fuel-air mixing to the extent that the flame length decreased by up to 30%, when certain shock locations and strengths were chosen that are optimum for the investigated geometry and operating conditions. The researchers reasoned that enhanced mixing resulted, in part, because the shocks induce radial inflows of air into the fuel jet. It was concluded that optimizing the mixing and stability limits for any combustor geometry requires careful matching of shock strengths and locations of shock/flame interaction.

In another investigation[10] shock-induced mixing was simulated numerically. Parallel flows of a heavy gas interspersed with other flows of a lighter one were overtaken

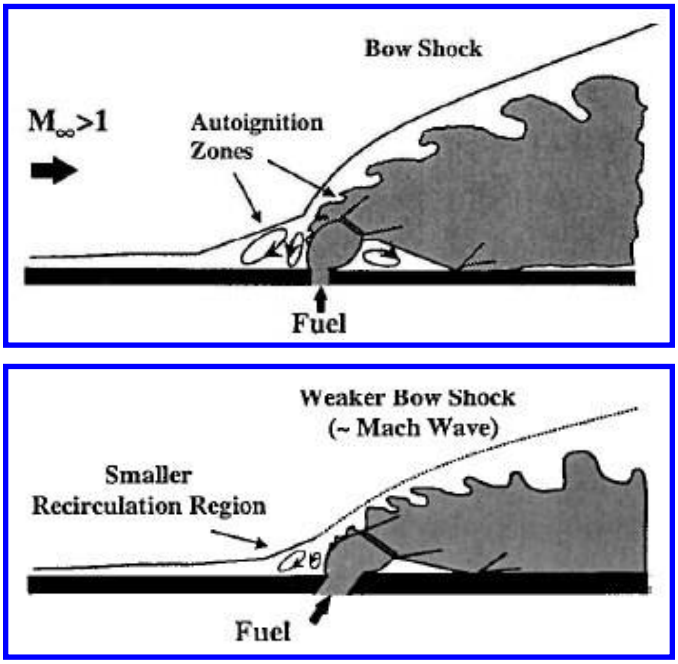

Figure 2. Traverse (top) and oblique injection (bottom), [5]

by a normal shock wave. It was shown that vorticity is generated at each location of interaction of the density gradient across each light/heavy interface with the shock wave pressure gradient. Since the pressure and density gradient vectors are out of phase at these locations, their cross-product ($\nabla p \times \nabla \rho$) has non-zero values. This cross-product defines the Baroclinic vorticity vector, $\partial_t \vec{\omega}_{bc} = (\nabla p \times \nabla \rho)/\rho^2$, which causes the light gas regions to roll up into one or more counter-rotating vortex pairs, stirring and mixing the light and heavy gases together. It was concluded that, whenever possible, multiple shock waves should be utilized.

Injection-induced shock wave formation in supersonic flows is an inevitable fact. Nevertheless, these shock waves have positive effects on fuel-air mixing and flame stabilization, when they interact with the air/fuel shear layer. Some beneficial effects of this interaction are: (a) directing the airflow locally towards fuel for increased entrainment rates, (b) creation of additional vorticity that enhances mixing, (c) elongation of the flame recirculation zones due to the adverse pressure gradient of a shock wave, and (d) increase in flow static pressure and temperature through a shock wave. The exact role of each effect needs further substantiation and quantification. This present work has the objective of numerically comparing the oblique and traverse configurations of fuel injection at different sets of operating conditions, from the points of view of efficiency and effectiveness. The goal is to achieve enhanced mixing while reducing injection-induced pressure losses.

II. Test Matrix and Simulation Assumptions

Since this current study utilizes a numerical approach, code validation and comparisons to actual experimental data were facilitated by choosing the normal-injection geometry of the experimental work of Balar et al.[11] This geometry is depicted here in Figure 3. The oblique configuration of fuel injection was added to facilitate a comparison between the traverse and oblique configurations. Both injection schemes share the capability of utilizing a non-intrusive wall injection port, without having to insert obstructive struts in the flowpath. Thus, the main objective of this study is to compare oblique to traverse injection from the points of view of mixing and injection-induced shock losses.

Air is supplied from a 5.1-cm pipe and accelerated subsonically through a convergent section to a square cross-sectional area of 1.27 x 1.27 cm^2. This 1.27-cm spanwise dimension of the flow passage maintains this value up to the test rig exit plane. The airflow is then further accelerated through a convergent-divergent (CD) nozzle. A quadrant of a disc 0.518 cm in diameter and 1.27 cm thick (i.e., spanning the entire flow passage) forms the convergent section of this nozzle, which results in a rectangular flow throat area of 0.752 x 1.27 cm^2. The nozzle divergent section was designed using the method of characteristics and expands the flow back to an area of 1.27 x 1.27 cm^2. The flow passage upper and lower walls then expand at 3.5° each for an axial distance of 3.8 cm to further accelerate the flow, keeping the spanwise dimension constant at 1.27 cm. Following the expansion is a fuel injection section, where the flow passage maintains a constant area of 1.735 x 1.27 cm^2 for 3.18 cm and terminates by the 0.318-cm injection port. To prevent choking and/or excessive blockage of the airflow, due to fuel injection, the flow passage upper and lower walls expand again, right after the injection port, at 3.5° each for 28.56 cm up to the test rig exit plane.

The ESI-Group CFD-FASTRAN 2007 LES-based code was used for all simulations presented here. A variable-sized grid was generated for the examined geometry with a total of about 207000 nodes. Tighter meshing was implemented near and at the critical geometry locations, e.g. convergent-divergent nozzle, fuel injection port, corners of expansion, etc. The mesh size varies from 0.25 mm down to 0.01 mm, in order to capture the flowfield critical features, such as shock waves and shear layers. Special emphasis was placed on the level of cell skewness. The flow passage was divided into six sub-volumes of regular geometrical shapes (i.e., pyramid frustums and parallelepipeds), with each volume meshed separately, in order to keep the skewness level of the most skewed cell below 0.5.

The Baldwin-Lomax turbulence model was implemented. Calculation of viscosity and conductivity was based on the kinetic theory of gases. The mass diffusivity was calculated based on Fick's law with a Schmidt number of 0.5. A turbulent Prandtl number of 0.9 was used for calculating the turbulent conductivity. The total pressure and temperature at the air inlet were kept fixed, so as to simulate the experimental conditions of Balar et al.,[11] where a total temperature of 300 K was maintained, and the total pressure was controlled by means of a regulator and monitored by a static pressure transducer. Thus, these two quantities of the air inlet were preserved throughout the iteration process in each case, until convergence was attained. A total temperature of 300 K was selected for the air inlet in all cases presented in this work. The total pressure was assigned the experimentally investigated values of 6.442 and 9.163 bar abs, which correspond to air mass flow rates of 0.146 and 0.204 kg/s, respectively, as calculated from the choked nozzle relations with a throat area of 0.752 x 1.27 cm^2.

Owing to the relatively large cross-sectional area of the air inlet, the entrance velocity of air was only 9.4 m/s, resulting in almost identical inlet stagnation and static conditions. Fuel

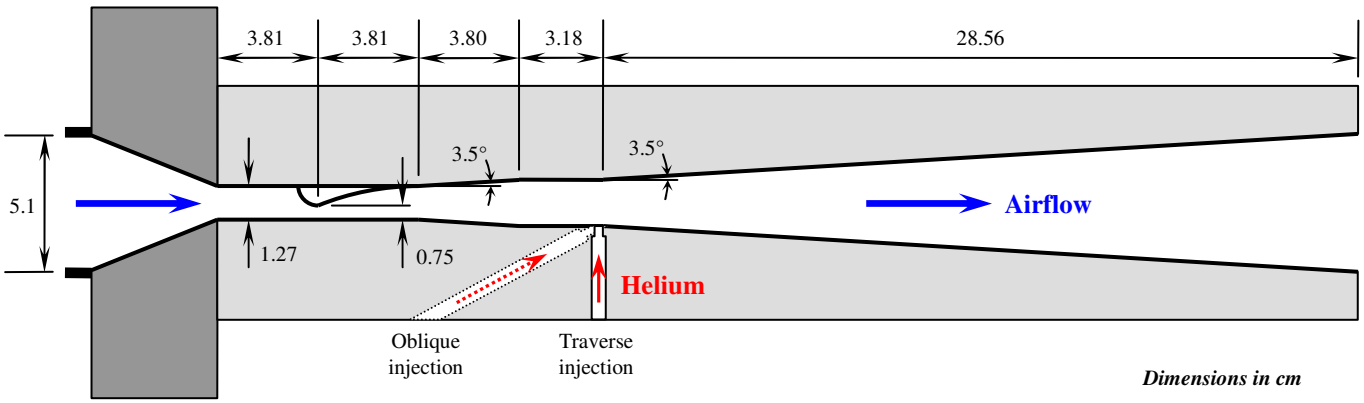

Figure 3. Schematic of the examined geometry

was simulated by helium, similar to what was done experimentally. Two mass flow rates of helium are investigated, namely 1.98 and 4.26 g/s. For both flow rates, the speed of injection is sonic, 883 m/s, at a total temperature of 300 K. Thus, the amount of injected helium is controlled solely by the total pressure of injection with values of 2.700 and 5.762 bar abs, respectively. The nozzle walls were set to be adiabatic, assuming insignificant heat transfer through the thick test rig steel walls.

The initial conditions of simulation were set equal to those of the air inlet for each case, i.e. velocity of 9.4 m/s and static temperature of 300 K. The static pressure, however, was set to 1 atm. Consequently, the simulation incorporated the transient flow behavior once the air supply valve is opened in the experimental test facility, allowing the high-pressure air to expand and "march" from inlet to exit. A total of 9000 iterations or cycles were set for each simulated case. Convergence was usually attained after 8000 – 8500 iterations. Table 1 lists the test matrix for the results presented here. Our main focus is to compare the oblique and traverse injection configurations. Nevertheless, the case of no fuel injection (#1) has also been included, in order to provide further validation of the numerical results with the corresponding experimental data.

III. Results and Discussion

Code Validation

A sample code-validation comparison is depicted in Figure 4, which shows the variation in static pressure along the flow passage upper wall (opposite to the fuel injection port) for cases 1 and 7. The static pressure values are normalized by the total pressure at the air inlet, while the axial location is normalized by the injection-port diameter (d = 0.318 cm).

Table 1. Test Matrix

Case	Air mass flow rate [kg/s]	Helium mass flow rate [g/s]	Configuration
1	0.204	0	—
2	0.146	1.98	Oblique (5°)
3			Traverse
4	0.146	4.26	Oblique (5°)
5			Traverse
6	0.204	1.98	Oblique (5°)
7			Traverse
8	0.204	4.26	Oblique (5°)
9			Traverse
10	0.204	5.95	Oblique (5°)

Good agreement is observed between the numerical and experimental results with and without fuel injection. Therefore, for the given geometry and operating conditions, the code is capable of capturing the fine features of the flowfield and providing credible simulation results.

Role of Injection Configuration

In order to examine the effect of injection configuration on combustor performance, cases 2 to 9 are compared to each other in Figures 5a – d, which pair them by the air and helium mass flow rates they share. Shown in Figure 5 are again the variations in static pressure along the upper wall (opposite to the fuel injection port). However, since multiple air flow rates are considered here, the static pressure variation of each case is normalized by the *case* total pressure at the air inlet. Figure 6 shows the Mach number profiles within the first 50 injection-port diameters downstream of the injection point, also for cases 2 to 9. Both figures reveal that the oblique configuration provides superior performance over the traverse one. Minor local peaks of pressure rise are observed downstream of the injection port for all cases of oblique injection. The traverse configuration, however, is accompanied by wide regions of elevated wall pressures upstream of the injection port, which indicates the presence of strong normal (or highly oblique) shock waves that raise the flow pressure considerably and decelerate it to subsonic speeds. Case 7, in Figure 5c, is an exception. It should be noted, however, that this case has the higher air flow rate and lower helium one. Thus, it can be concluded in this case that the airflow was more "powerful"

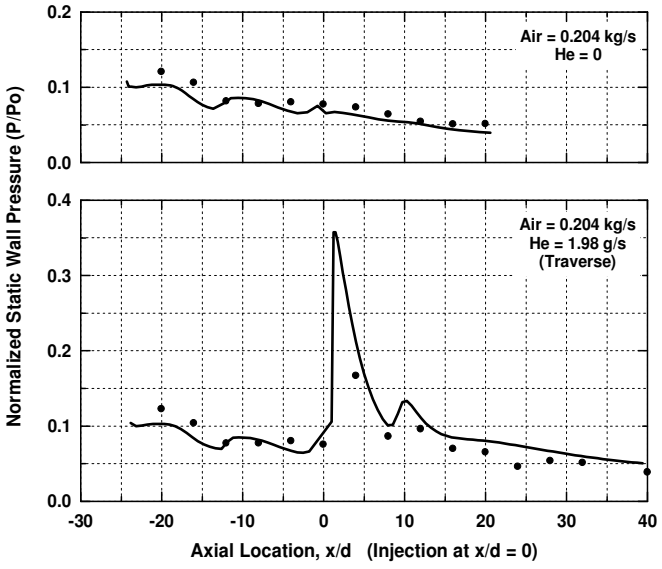

Figure 4. Static pressure variation along the flow passage upper wall (opposite of fuel injection port); pressure normalized by the total pressure at the air inlet; axial location normalized by injection-port diameter (d = 0.318 cm). ●, experimental results (Balar et al. [11]); ——, simulation results (present study)

in resisting the penetration of helium, and thus shocked with a weaker and less oblique wave, see Figure 6. Following the same methodology, when more helium is injected (Figure 5d), the airflow shocks more severely. A similar, intermediate level of pressure rise is observed in Figure 5a, wherein both the air and helium flow rates are low. Pairing the lower airflow and higher helium one, however, results in the highest level of pressure rise, see Figure 5b.

The smaller local peaks of pressure rise, which are characteristic of oblique injection, are attributed to weaker oblique shock waves, of smaller wave angles, that reflect up and down between the opposite upper and lower walls. In

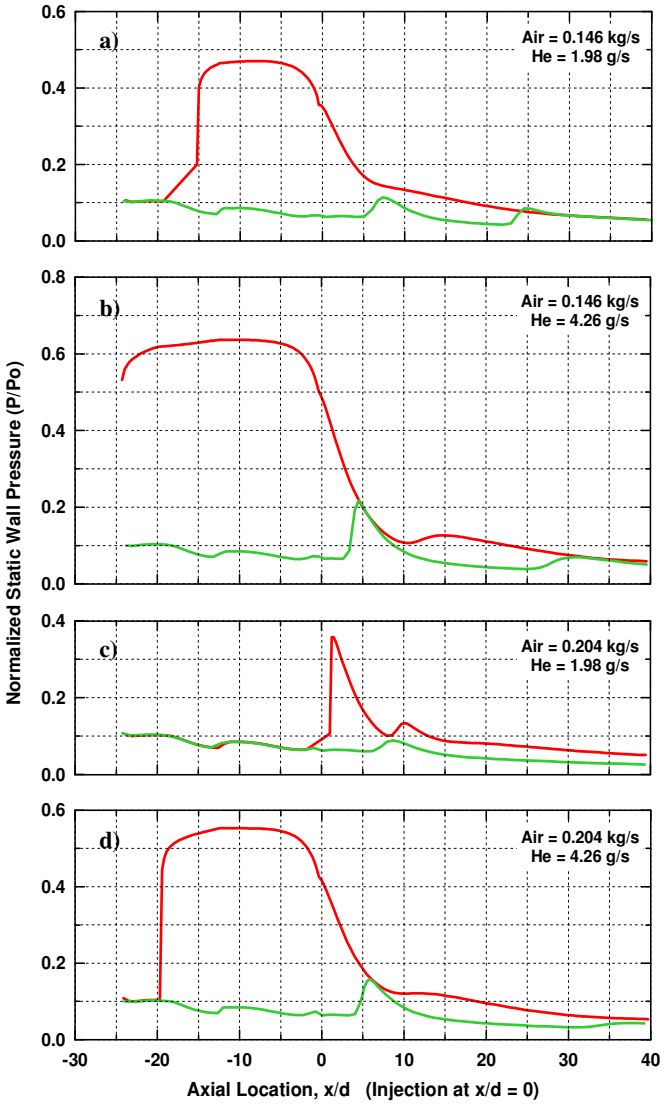

Figure 5. Static pressure variation along the flow passage upper wall (opposite of fuel injection port); pressure normalized by the *case* total pressure at the air inlet; axial location normalized by injection-port diameter (d = 0.318 cm). Green, oblique; red, traverse injection

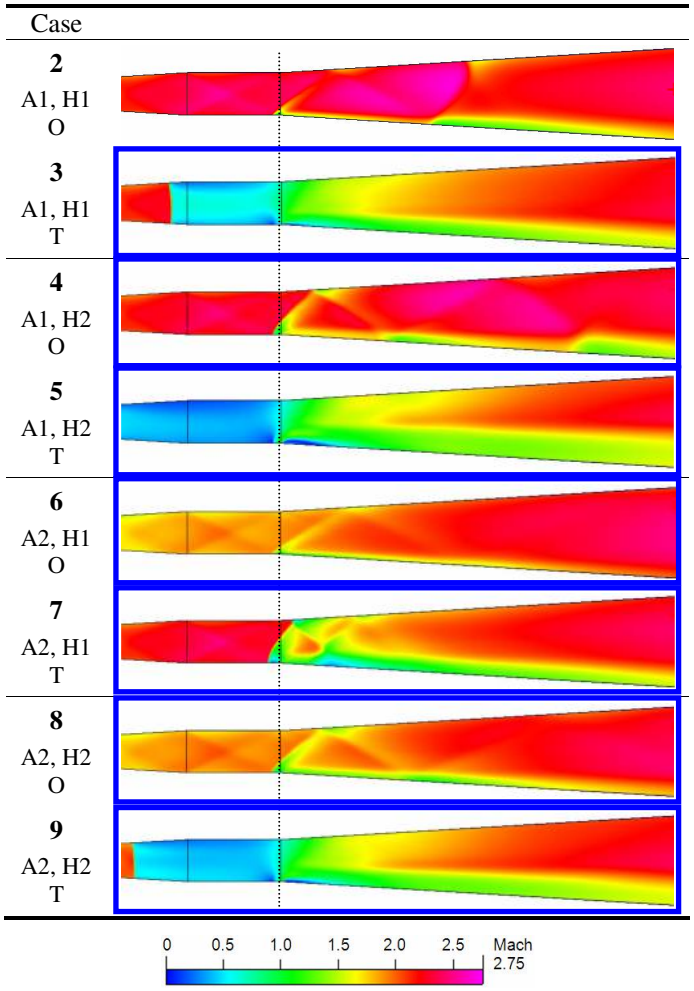

Figure 6. Mach number profiles within the first 50 injection-port diameters downstream of the injection point for cases 2 to 9. Vertical dashed through-line represents location of injection. A1, A2 = air flow rates of 0.146 and 0.204 kg/s, respectively; H1, H2 = helium flow rates of 1.98 and 4.26 g/s, respectively. O, Oblique; T, Traverse.

fact, the smaller angles of those shock waves are the reason why they are capable of reflection, whereas the normal (or highly oblique) waves of traverse injection cannot, see Figure 6. It should be noted here that a train of weaker oblique shock waves is still favorable over a single strong normal wave. The latter imposes a higher level of total pressure loss on the flow and decelerates it to subsonic velocities, whereas the Mach number downstream of an oblique shock train is still supersonic.

The regions of elevated wall pressures accompanying traverse injection in Figure 5 represent the bifurcation zones of the upstream normal shock waves as they intersect with the boundary layer. A wider bifurcation zone means a thicker boundary layer and a stronger shock wave. These are two negative side effects associating traverse injection,

because the airflow (i) suffers from blockage due to the thick boundary layer and (ii) loses total pressure significantly through the normal shock wave. A clear example is case 5, where the bifurcation zone spans 20 injection-port diameters, as seen in Figure 5b. Bifurcation zones are also known for a third negative side effect, namely boundary layer separation and the consequent creation of a "hot spot" within the legs of a bifurcated shock wave—a phenomenon that is undesirable and should be avoided/eliminated, whenever possible.

To further strengthen the findings made from Figures 5 and 6, the variation in fuel (helium) mass fraction along the lateral direction was plotted at four different streamwise locations downstream of the injection port for both injection configurations. Cases 2 to 5, sharing the smaller air flow rate (0.146 kg/s), were chosen for this comparison. Figure 7 compares cases 2 and 3, with a common helium flow rate of 1.98 g/s. Figure 8, on the other hand, compares cases 4 and 5 that share the higher helium flow rate of 4.26 g/s. It is worth noting here that a similar analysis was conducted for the higher air flow rate (0.204 kg/s) but is not presented here, because both analyses yielded the same conclusions. This statement is concurred by Figure 9, where the helium mass fraction profiles are plotted from the injection port to the exit plane for cases 2 to 9. It can be seen that cases 2 to 5, sharing the 0.146-kg/s air flow rate, behave qualitatively similar to cases 6 to 9 with an air flow rate of 0.204 kg/s, from the points of view of injection configuration and amount of injected helium.

Referring back to Figures 7 and 8, the most remarkable observation is that the helium mass fractions associated with oblique injection are significantly lower than those of traverse injection at *all* lateral as well as streamwise locations. The four streamwise locations x/d = 10, 20, 50, and 90 (exit plane), chosen for display in Figures 7 and 8, are just sample locations of an entire flowfield downstream of the injection port, where this trend was found to prevail at every streamwise location all the way down to the exit plane. Oblique injection provides lower helium mass fractions everywhere and not just close to the injection port. It was expected to see higher helium mass fractions accompanying the traverse configuration close to the injection port, i.e., at x/d = 10 (Figures 7a and 8a). This is attributed to the fact that helium is injected traversely away from the wall, which enables it to penetrate the crossflow of air to greater depths. It should be noted, however, that the difference in jet penetration is only about 20% of the flow passage height at the location of injection. Thus, in contrast with the common misconception, achieving higher levels of jet penetration does not necessarily mean better fuel mixedness.

Figures 7 and 8 also reveal that the mass fractions of helium decay at a much slower rate for the cases of traverse injection as compared to those of oblique injection. Thus, from the point of view of mixing, oblique injection shows a superior performance over traverse injection. This negates some of the findings of previous research,[1,5,6] which state

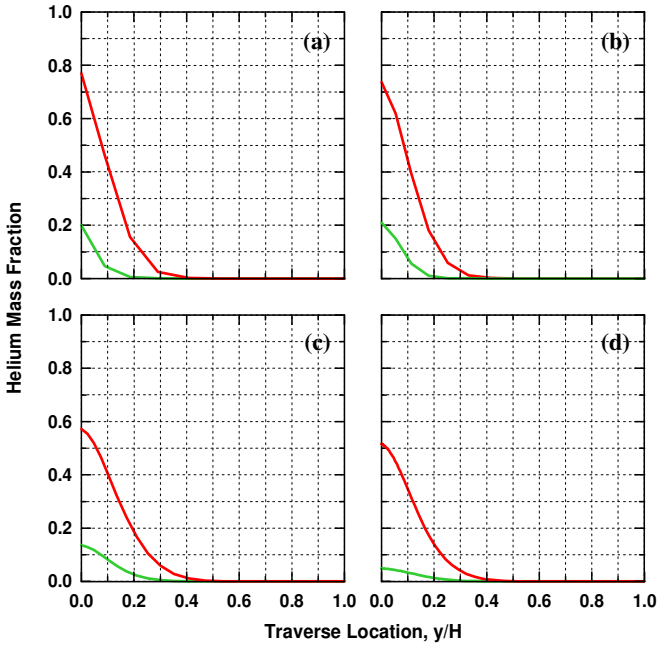

Figure 7. Variation of helium mass fraction along the traverse direction at four streamwise locations downstream of the injection port. Air flow rate = 0.146 kg/s, helium flow rate = 1.98 g/s. Green, oblique; red, traverse injection. H, height of the flow passage at the corresponding axial location
(a) x/d = 10, H = 2.12 cm, (b) x/d = 20, H = 2.51 cm,
(c) x/d = 50, H = 3.68 cm, (d) x/d = 90 (exit plane), H = 5.23 cm

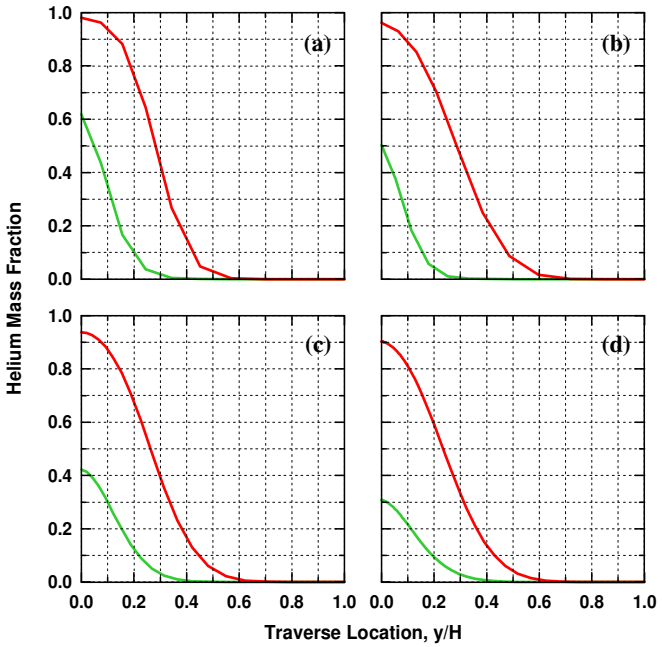

Figure 8. Variation of helium mass fraction along the traverse direction at four streamwise locations downstream of the injection port. Air flow rate = 0.146 kg/s, helium flow rate = 4.26 g/s. Green, oblique; red, traverse injection. H, height of the flow passage at the corresponding axial location
(a) x/d = 10, H = 2.12 cm, (b) x/d = 20, H = 2.51 cm,
(c) x/d = 50, H = 3.68 cm, (d) x/d = 90 (exit plane), H = 5.23 cm

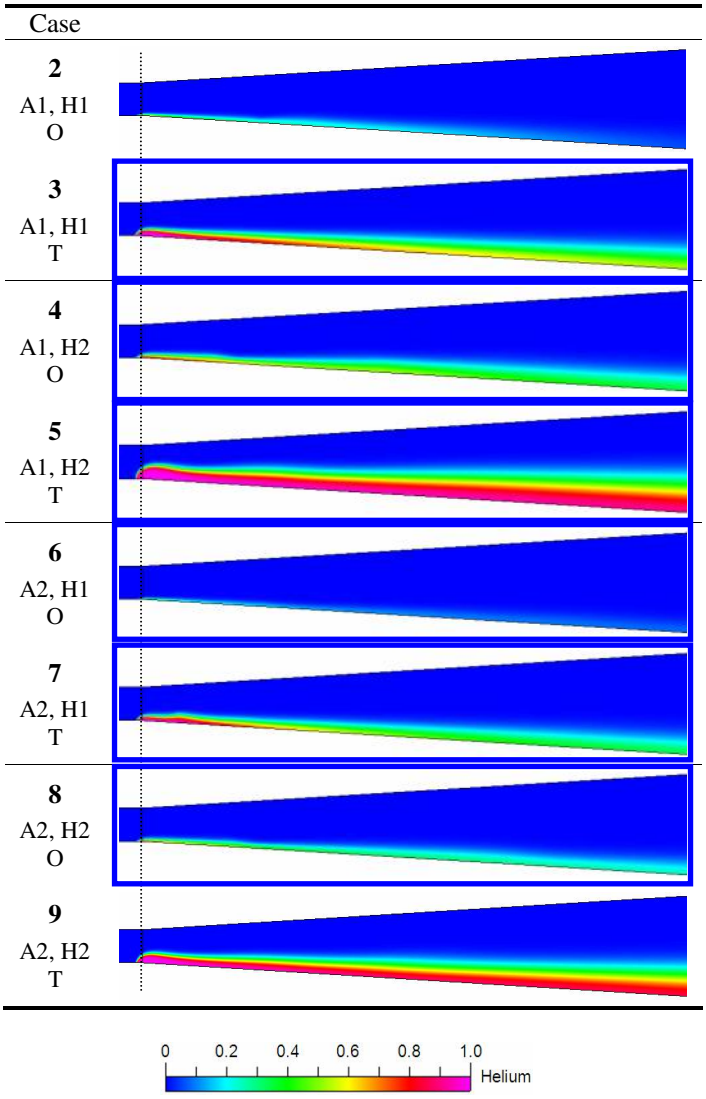

Figure 9. Helium mass fraction profiles from the injection port (x/d = 0) to the exit plane (x/d = 90) for cases 2 to 9. Vertical dashed through-line represents location of injection port. A1, A2 = air flow rates of 0.146 and 0.204 kg/s, respectively; H1, H2 = helium flow rates of 1.98 and 4.26 g/s, respectively. O, Oblique; T, Traverse.

that traverse injection is most favorable for supersonic flows. Even at the exit plane, which is 90 injection-port diameters downstream of the injection point, oblique injection still results in a better fuel mixedness, with a wall helium mixture fraction one order of magnitude less than that of traverse injection (see Figure 7d). Thus, it can be concluded from the comparisons of Figures 7, 8, and 9 that oblique injection is more effective in achieving better mixing over both the near- and far-field regions. Injection at small oblique angles was proven superior over both the parallel and traverse configurations in our previous work, Abdelhafez et al.[12] The results of both studies agree well, although the studied geometries are different.

To summarize the role of injection configuration, the mixing lengths of cases 2 to 10 (see Table 1) are listed in Table 2. A few important remarks should be pointed out here. First, the mixing length (L) is defined as the streamwise distance from the injection port to the cross-section, where the helium mass fraction at the lower wall has decayed to an arbitrarily chosen value of 0.2. Second, all mixing lengths, listed in Table 2, are normalized by the injection-port diameter (d = 0.318 cm). Finally, case 10 shares the 0.204-kg/s air flow rate with cases 6 to 9 but has a new helium flow rate of 5.95 g/s, tailored to yield an equivalence ratio equal to that of case 4. This facilitates an analysis at constant equivalence ratio, as will be shown later. It can be observed from Table 2 that the mixing lengths of all traverse-injection cases extend beyond the test rig exit plane (x/d = 90). On the other hand, oblique injection provides a substantially better performance, evidenced in the smaller mixing lengths of its cases.

Shock/Shear Layer Interaction

As the analysis of the role of injection configuration has shown, oblique injection provides an optimum solution of the injection problem that incorporates many demanding yet conflicting parameters. These parameters include increasing the injection system efficiency as well as effectiveness, and alleviating the problem of hot spots. The reason behind this superior behavior of oblique injection is that it benefits most from the phenomenon of shock/shear layer interaction.[12,13] This is proven in Figure 10, where the profiles of Mach number and lateral velocity component (V, m/s) of case 4 are depicted. This component of velocity highlights any lateral motion of any of the two fluids, air and fuel. Case 4 has been particularly chosen, because it gives the clearest demonstration of the existence of shock/shear layer interaction at multiple locations in the flowfield.

When a shock wave impinges on the shear layer between two mixing flows, it causes significant spreading of that shear layer downstream of the region of impingement.[13] The Mach number profiles, shown in Figure 10, support this statement. Locations 1 and 2 are clear examples of how the

Table 2. Mixing Length

Fuel flow rate [g/s]	Mixing Length, L/d (d = 0.318 cm)			
	Air = 0.146 kg/s		Air = 0.204 kg/s air	
	Oblique	Traverse	Oblique	Traverse
1.98	26	> 90	5.5	> 90
4.26	85	> 90	70	> 90
5.95			87	

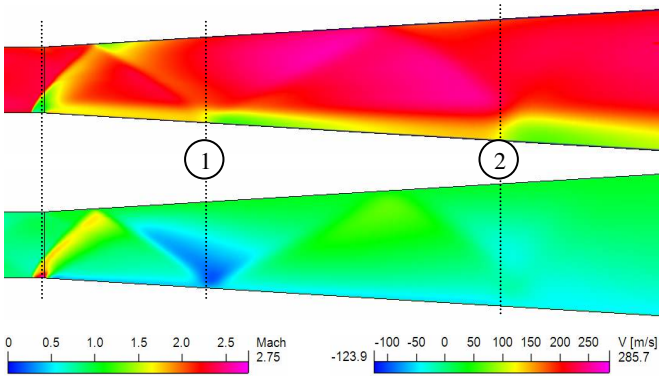

Figure 10. Mach number (top) and lateral velocity component (bottom) within the first 50 injection-port diameters downstream of the injection point for case 4, air flow rate = 0.146 kg/s, helium flow rate = 4.26 g/s, oblique injection. First vertical dashed through-line on the left represents location of injection port.

air/fuel shear layer spreads as a result of its interaction with the airflow shock train. Note that the lateral component of velocity has significant negative values at locations 1 and 2. Thus, it can be deduced that the airflow is being forced down into the fuel flow, due to induced vorticity[10] at the shock/shear layer interaction region, where roll-up vortices stir and mix both flows. This explains the superior behavior of oblique injection, in spite of the compressible nature of supersonic airflows, which makes them resistive to penetration and mixing. It should be noted, however, that the magnitude of shear layer spreading is small enough not to cause significant blockage of the core airflow. A close investigation of the Mach number profiles in Figure 10 shows that the shear layer spreads only locally, for a few injection-port diameters downstream of each interaction region (locations 1 and 2), before the core flow recovers and further expands, suppressing the shear layer back to smaller thicknesses.

Effect of Equivalence Ratio

The following analysis of the effect of equivalence ratio will be limited to oblique injection only, i.e., even-numbered cases in Table 1. Figure 11 shows a plot of the different mixing lengths, listed in Table 2, versus their corresponding equivalence ratios. It can be observed that the mixing length increases with equivalence ratio. However, their relationship is not linear. The curve starts with a positive second derivative (i.e., increasing slope), exhibits an inflection point at an equivalence ratio of about 0.5, then continues with a decreasing slope. Plausible explanations of these trends can be extracted from Figure 12, which shows the Mach number profiles of cases 2, 4, 6, and 8, depicted in the order of their equivalence ratios. In addition to the fact that all four cases have similar flow structures, it should be noticed that the strength of the injection-port shock wave increases with increasing equivalence ratio. The angle of this shock wave is considered a measure of its strength. Since the reflections of weaker (i.e., less oblique) shock waves are known to be more susceptible to the details of the examined geometry (as explained in Figure 13), large relative changes in mixing length are expected in the region of equivalence ratios containing cases 2 and 6. This explains the increasing slope of the mixing length / equivalence ratio curve in this region. Stronger shock waves, on the other hand, are less sensitive to the geometry details. Consequently, smaller relative changes in mixing length are characteristic of the region of equivalence ratios containing cases 8 and 4, which explains the decreasing slope in this region.

Figure 11 also shows that larger mixing lengths are necessary at higher equivalence ratios, as expected. Increasing the equivalence ratio means that more fuel has to be mixed with a unit of airflow, which demands larger mixing lengths. The effects of decreasing the air flow rate or injecting more fuel are similar. The core airflow loses total pressure in both situations, because the injection-induced shock waves gain strength. It should be noted, however, that these trends observed in Figures 11 and 12 are expected to change substantially, if the injection angle is varied, because it is a parameter of primary importance in controlling the strength of injection-induced shock waves.

Another important finding of Figure 11 is that cases 4 and 10 have equal equivalence ratios and almost the same mixing lengths, which suggests that the mixing length depends

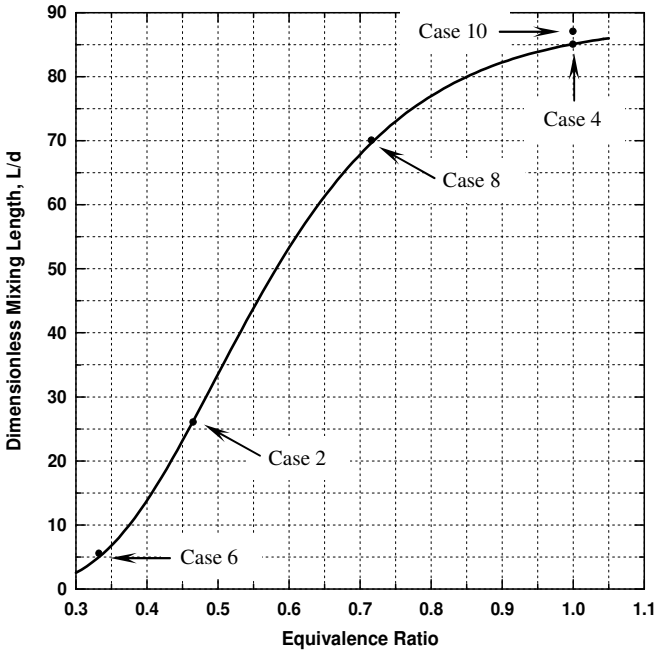

Figure 11. Variation in mixing length with equivalence ratio for the cases of oblique injection (5°). Mixing length normalized by injection-port diameter (d = 0.318 cm)

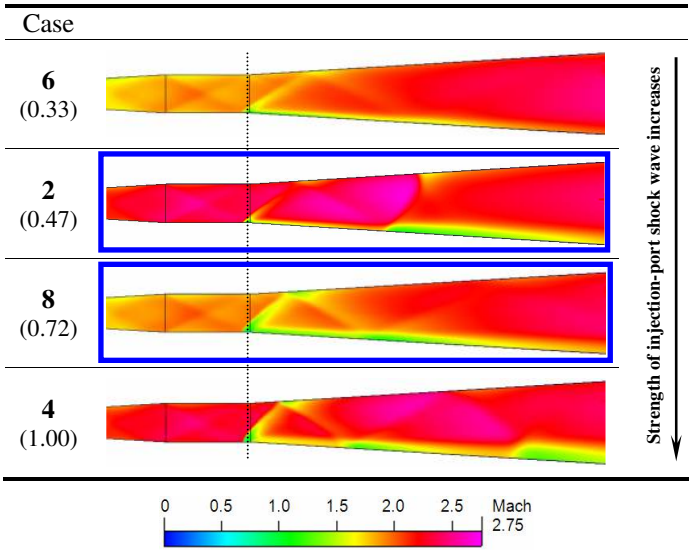

Figure 12. Mach number profiles within the first 50 injection-port diameters downstream of the injection point for cases 6, 2, 8, and 4. Vertical dashed through-line represents location of injection port. Value of equivalence ratio of each case is written in parentheses below the case number

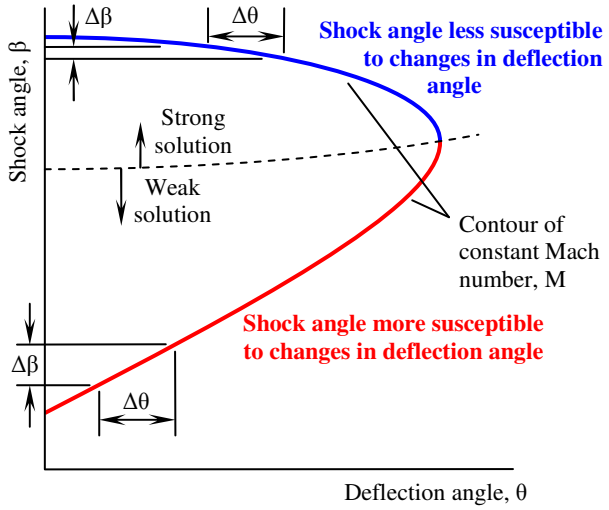

Figure 13. Schematic of θ-β-M diagram of oblique shock waves

primarily on equivalence ratio, if the injection angle is kept constant. This statement is concurred by Figure 14, where the Mach number profiles of cases 4 and 10 are compared within the first 50 injection-port diameters downstream of the injection point. Considerable similarity in flow structure can be observed, which explains why the mixing lengths are almost identical. However, it should be noted here again that these trends are expected to change, if the injection angle is varied, for the same reasons mentioned earlier.

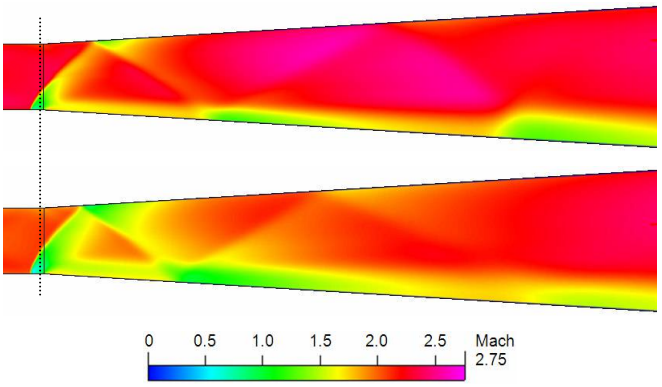

Figure 14. Mach number profiles within the first 50 injection-port diameters downstream of injection point for cases 4 and 10. Vertical dashed through-line represents location of injection

Choice of Injection Angle

Having demonstrated that fuel injection at small oblique angles is more favorable over traverse injection for supersonic airflows, the questions that arise at this point are: Why the choice of a 5° angle of oblique injection in this work? If the injection angle should change to adapt to variable operating conditions, how much change is necessary? What is the optimum range of injection angles? What are the criteria and parameters governing the choice of an angle within such range? Answering all these questions in detail is beyond the scope of this study. Nevertheless, some preliminary answers and thoughts will be provided here. The 5° angle was chosen for all oblique-injection cases of this work, because this angle showed superior performance over all other angles investigated in our previous work.[12] In spite of the differences in geometry and operating conditions, those findings were considered a practical guideline for this study. However, in order to provide accurate answers to the remaining three open questions, extensive computational analyses, supported by experimental validation, are needed. The matrix of governing parameters is considerably wide and involves, but is not limited to, (a) properties (i.e., Mach number, pressure, temperature, and flow rate) of the incoming airflow as well as those of fuel, (b) injection-port size (relative to the combustor dimensions in its vicinity), and (c) flow passage geometry and dimensions, especially downstream of the injection point. These parameters might have different effects, of varying degrees of significance, on the choice of an optimum injection angle. Nevertheless, they all affect the shock/shear layer interaction mechanism that distinguishes oblique injection and is of vital importance for achieving good mixing in supersonic flows.

Although extensive computational as well as experimental work is still needed to quantify the choice of injection angle accurately, some important semi-quantitative guidelines can still be drawn from our present results. The range of optimum angles is expected to be narrow. It extends from

close to parallel up to about 15° only, because of the following reasons. (a) The average Mach number over the entire cross-section of a scramjet combustor is about 3.5 (calculated roughly for a hypersonic vehicle flying at Mach 10). Referring to the θ-β-M diagram of oblique shock waves, the maximum deflection angle for this Mach number is about 37°, beyond which the flow forms a severe detached bow-shock that is usually capable of decelerating it to subsonic Mach numbers over the entire combustor height, especially at high injection velocities in high-aspect-ratio combustors. Thus, in order to minimize the shock losses accompanying injection, small angles should be utilized. (b) The Mach number close to the wall, where the injection port is located, is definitely lower than that of the core flow, which puts more restriction on the injection angle to avoid bow-shock formation. (c) The incoming flow to a scramjet combustor is not shock-free. On the contrary, this flow has passed through the vehicle inlet and isolator sections, where considerable shock formation and boundary layer growth takes place. Based on the results of this work and those of other previous studies,[9] it was shown that few weak oblique shock waves is all what it takes to achieve good mixing and flame holding at small angles of injection. Thus, any minor shocks, still present in the combustor after the inlet and isolator sections, will simply be sufficient enough to avoid imposing strong additional shocks on the flow due to fuel injection. Consequently, small oblique injection angles are recommended.

IV. Conclusions

The oblique and traverse configurations of fuel injection in scramjet combustors are compared to each other in this study through a series of simulations that yielded the following conclusions. (a) Injecting fuel obliquely results in better near- and far-field mixing, as compared to traverse injection. (b) Full penetration of supersonic flow is not possible, even with traverse injection. Thus, penetration should not be considered as a measure of fuel mixedness. (c) Oblique injection induces few weak oblique shock waves that interact with the air/fuel shear layer downstream of the injection point to achieve the necessary mixing. Induced vorticity is generated at the locations of shock/shear layer interaction. Together with the adverse pressure gradient across each shock wave, this vorticity aids in mixing the air and fuel streams across their shear layer. Traverse injection lacks such beneficial interaction, as the flow undergoes a single severe normal, or highly oblique, shock wave (i.e., incapable of reflection) upstream of the injection port. (d) Oblique injection is recommended, as it provides better performance from the points of view of mixing, total pressure loss, flow blockage, and boundary layer separation. (e) At constant injection angle, the structure of a non-reacting flowfield depends strongly on equivalence ratio. This structure, in turn, influences the mixing length significantly. Thus, the equivalence ratio can be considered as the sole controlling parameter of mixing length. (f) The choice of injection angle depends on many parameters, such as the physical properties of both air and fuel flows and the details of the geometry under investigation.

Acknowledgments

This work was supported by the Space Vehicle Technology Institute under grant NCC3-989 jointly funded by NASA and DoD within the NASA Constellation University Institutes Project, with Claudia Meyer as the Project Manager. The DoD work was supported by the USAF and is gratefully acknowledged.

The simulation code, CFDRC, was provided by ESI-Group. This support is gratefully acknowledged.

References

[1]Gruber, M.R., Nejad, A.S., Chen, T.H., and Dutton, J.C., "Mixing and Penetration Studies of Sonic Jets in a Mach 2 Freestream," Journal of Propulsion and Power, Vol. 11, No. 2, March-April 1995.

[2]Kutschenreuter, P., "Supersonic Flow Combustors," Scramjet Propulsion, edited by Curran, E.T. and Murphy, S.N.B., Progress in Astronautics and Aeronautics Series, Vol. 189, 2000, pp. 513 – 567.

[3]Sung, C. J., Li, J. G., Yu, G., and Law, C. K., "Chemical Kinetics and Self-Ignition in a Model Supersonic Hydrogen–Air Combustor," AIAA Journal, Vol. 37, No. 2, February 1999, pp. 208 – 214.

[4]Conaire, M. O., Curran, H. J., Simmie, J. M., Pitz, W. J., and Westbrook, C. K., "A Comprehensive Modeling Study of Hydrogen Oxidation," International Journal of Chemical Kinetics, Vol. 36, Issue 11, pp. 603 – 622.

[5]Ben-Yakar, A., "Experimental Investigation of Transverse Jets in Supersonic Cross-flows," Ph.D. Dissertation, Dept. of Mechanical Eng., Stanford Univ., Stanford, CA, Dec. 2000.

[6]Huber, P. W., Schexnayder, C. J., and McClinton, C. R., "Criteria for Self-Ignition of Supersonic Hydrogen-Air Mixtures," NASA TP 1457, 1979.

[7]Ben-Yakar, A., and Hanson, R. K., "Experimental Investigation of Flame-Holding Capability of a Transverse Hydrogen Jet in Supersonic Cross-Flow," Proc. Twenty-Seventh Symposium (Intl.) on Combustion, The Combustion Inst., Pittsburgh, PA, 1998, pp. 2173 – 2180.

[8]Lee, S. H., "Characteristics of Dual Transverse Injection in Scramjet Combustor," Journal of Propulsion and Power, Vol. 22, No. 5, September–October 2006, pp. 1012 – 1019.

[9]Huh, H., and Driscoll, J. F., "Measured Effects of Shock Waves on Supersonic Hydrogen-Air Flames," 32nd Joint Propulsion Conference and Exhibit, Lake Buena Vista, FL, July, 1996, AIAA- 96-3035.

[10]Yang, J., Kubota, T., and Zukoski, E. E., "Applications of Shock-Induced Mixing to Supersonic Combustion," AIAA Journal, Vol. 31, No. 5, May 1993, pp. 854 – 862.

[11]Balar, R., Young, G., Pang, B., Gupta, A. K., Yu, K. H., and Kothari, A. P., "Comparison of Parallel and Normal Fuel Injection in a Supersonic Combustor," 42nd AIAA/ASME/SAE/ASEE Joint Propulsion Conference and Exhibit, Sacramento, California, July 9-12, 2006, AIAA-2006-4442.

[12]Abdelhafez, A., Gupta, A. K., and Yu, K. H., "Interaction of a Gaseous Fuel Jet with Shock-Wave-Rich Airflow," 45th AIAA Aerospace Sciences Meeting and Exhibit, Reno, Nevada, 8 – 11 Jan 2007, AIAA-2007-0390.

[13]Menon, S., "Shock-wave-induced mixing enhancement in scramjet combustors," AIAA 27th Aerospace Sciences Meeting, Reno, NV, Jan 1989, AIAA-89-0104.